JPE 7-3-3

A Novel Control Strategy for a Three-Phase Rectifier with High Power Factor and Stable Output Voltage

Hong-Hee Lee†, Van-Tung Phan*, Brovanov Sergey** and Tae-Won Chun*

†*School of Electrical Engineering, University of Ulsan, 680-749 Muger2dong-Namgu, Ulsan, Korea
**Dept. of Power Electronics, Novosibirsk State Technical University, Russia

ABSTRACT

In this paper, a proposed approach to improve the power factor of three-phase rectifiers and to stabilize the output voltage against load change is presented. The key elements of the given control strategy are small size, low cost, high performance, and simplicity. The proposed control strategy of switches is based on a prototype of three bi-directional switched consisting of four diodes and one IGBT. A control technique and operational procedure are also developed, both theoretically and experimentally. The experimental results clearly verify the theoretical analysis from the prototype connected to grid unity.

Keywords: Power factor, three-phase rectifiers, AC-DC converter

1. Introduction

A majority of the power electronics applications such as adjustable speed ac motors and dc servo motor drives, uninterruptible power supplies (UPS), battery storage, switching dc power supplies, and so on, use uncontrolled rectifiers which employ a three-phase bridge with diodes to interface to the ac power supplies. However, the diode bridge rectifier interconnected to the utility grid has a non-sinusoidal input current and a poor input power factor, which leads to lower performance of the power converters. Therefore, the necessity to develop a control strategy for the three-phase rectifiers in order to improve the power factor and achieve further overall cost reduction and high efficiency of the system has increasingly been emerging as a leading issue in power electronic fields.

To overcome the drawbacks mentioned above, a number of new techniques have been proposed for improving the power quality and the power factor of the three-phase rectifiers. According to [1], an ac to dc with a front-end three-phase rectifier with diodes and three boost inductors at the ac side which gives small reactive power is presented. Although the proposed method draws ac sinusoidal current and obtains almost unit power factor, the restriction of this method is that it is actually more difficult and challenging to design the boost switches in high power applications. Furthermore, one of the most prominent methods is to consider the rejection into the ac line with the third harmonic current, which results in a power factor close to that of a utility grid and gives almost sinusoidal input current in rectifiers. In [2], the third

Manuscript received Dec. 27, 2006; revised March 15, 2007
†Corresponding Author: hhlee@mail.ulsan.ac.kr
Tel: +82-52-259-2187, Fax: +82-52-259-2186, Univ. of Ulsan
*School of Electrical Engineering, Univ. of Ulsan
**Dept. of Power Electronics, NSTU, Russia

harmonic is created for the dc side by using two step-up dc-dc converters within a dc link in prototype. Another procedure presented in [3] is that the proposed circuit includes the interconnection of a delta-zig- zag transformer between the ac and dc side of the diode rectifier. However, there are some limitations to high power applications due to increasing the cost, size and weight of the magnetic components and related interfaces.

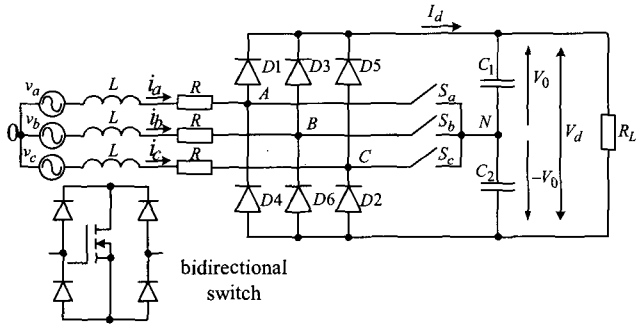

Fig. 1 Circuit of three-phase diode bridge rectifier and bidirectional switch

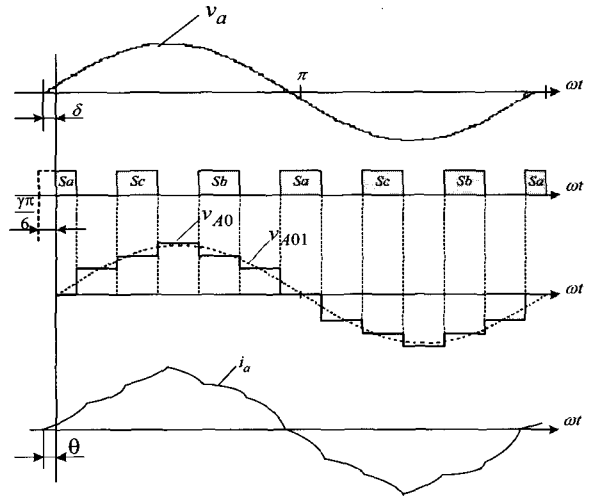

Fig. 2 Main waveforms of the proposed control strategy

On the other hand, a different approach is proposed in [4], which uses the harmonics elimination PWM techniques to improve the output voltage waveform whereas in [5] a circuit of an add-on simple cell with line-frequency commutated ac switches is applied. However, that converter does not fully investigate the proposed circuit's potentiality.

In this paper, although the structure of the prototype is the same as [6], [7], we present a new control method with additional switches that has better characteristics as follows: lower total harmonic distortion for small input current, higher input current performance over a small range of output power, and shorter settling time when the load is changed. The proposed scheme is simulated and verified experimentally.

2. Circuit configuration

The circuit shown in Fig. 1 consists of a three-phase diode bridge rectifier, and three bidirectional switches (S_a, S_b, S_c) that can be built by using one MOSFET or IGBT, and four diodes. The bidirectional switches are connected between the common neutral point (N) and the phase terminal (A, B, C).

It is assumed that the anode-to-cathode voltage of each diode of the rectifier as well as the voltage drop through bidirectional switches is of negligible quantity. Fig. 2 shows the waveforms of the considered power circuit.

The bidirectional switches, S_a, S_b and S_c, are turned on at an appropriate interval, conducting a partial line current. As a result, the input voltages v_{AO} , v_{BO} , v_{CO} - the voltages between each input terminal (A, B, C) and the zero point of the main source - become the staircase waveforms, and the input current waveforms become similar to the sinusoidal input voltages, in this case, it is clear that the power factor is improved.

In Fig. 2, the characteristics of the rectifier can be controlled by adjusting the parameters such as γ and δ, where γ is a constant value between 0 and 1 which determines the pulse width for S_a, S_b, S_c, and δ is the phase angle between the supply voltage and the fundamental component of the rectifier input voltage. Therefore, we can improve the characteristics of the considered rectifier by selecting a suitable γ and δ. In essence, this is the control strategy that uses a control technique of angle δ to improve system performance behavior.

3. The proposed control method

Fig. 3 shows an equivalent circuit and a phase diagram for fundamental components of the voltages and currents,

where V_a is the rms-value of the sinusoidal supply voltage, V_{A01} is the rms-value of the fundamental component of the input voltage of the rectifier, I_{a1} is the rms-value of the fundamental component of the input current of the rectifier, L is the input inductance including a leakage inductance of transformer - L_{lt} and an inductance of the inductor - L_i, and R is the input resistance.

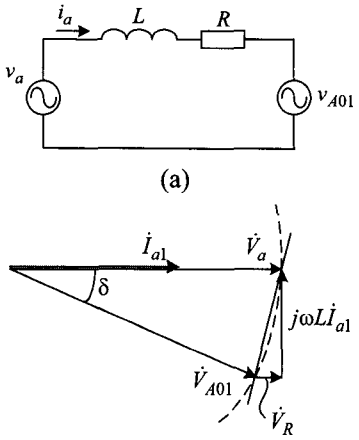

Fig. 3 Equivalent circuit and phase diagram for the fundamental components

The Fourier expansion of v_{A0} depicted in Fig. 2 gives the following equation

$$V_d = \frac{3\pi V_{A01}}{\sqrt{2}\left\{2\cos\left(\frac{\gamma\pi}{6}\right)+\cos\left(\frac{\pi}{3}-\frac{\gamma\pi}{6}\right)+\cos\left(\frac{\pi}{3}+\frac{\gamma\pi}{6}\right)\right\}} \quad (1)$$

We can control the output dc voltage V_d by using a parameter such as γ. The control of dc voltage by using γ is presented in [7]. In this case, however, we propose a novel approach in which the rectifier achieves the unit displacement factor (DF) and the output voltage V_d is almost stable at that time.

To obtain the unit displacement factor, the $\dot{I}_{a1}$ vector must be the same direction with the vector $\dot{V}_a$ regardless of the load. The output voltage V_d is absolutely stable in the case when the vector $\dot{V}_{A01}$ moves in an arc of the circle trajectory, as shown in Fig 3 (b). In this case, however, the current $\dot{I}_{a1}$ can not be in co-phase with the voltage $\dot{V}_a$. Therefore, instead of the arc of the circle, we can use a line which could be a boundary from the dropped voltage on an input resistance R. The angle $\delta = \theta = \gamma\pi/6$ is the maximum angle when current $\dot{I}_{a1}$ is in co-phase with the voltage $\dot{V}_a$ as shown Fig. 2. The θ is the angle between the fundamental component of the input current and the fundamental component of the input voltage.

Assuming that

$$\gamma = 0.5 \text{ and } V_{A01}(at\ \delta = \frac{\gamma\pi}{6}) = V_{A01}(at\ \delta = 0) \quad (2)$$

In this case, the smallest voltage $V_{A01(\min)}$ will be at the point $\delta/2$, we have $\frac{V_{A01(\min)}}{V_{A01}} = \cos(\frac{\pi}{24}) = 0.991$

Therefore, using control of δ when the end of the vector slides on the line which is the boundary from dropped voltage $\dot{V}_R$, we can obtain the output dc voltage changing 0.9% only.

When the fundamental input current I_{a1} is in co-phase with the voltage V_a the following equation can be obtained from Fig. 3 (b).

$$\delta = \arctan\left(\frac{\omega L I_{a1}}{V_a - V_R}\right) = \arctan\left(\frac{\omega L I_{a1}}{V_a - I_{a1}R}\right) \quad (3)$$

In practice for the control system, it is better to use the dc current instead of the alternating current I_{a1} for computing in an experiment. Thus, we need to change the current I_{a1} in equation (3) to the dc current I_d.

According to the analysis of the six operating modes described in [5], the next equation can be achieved below:

$$I_{a1} = \frac{I_d}{k\cdot\cos\delta} \quad (4)$$

where $k = \frac{3\sqrt{2}}{\pi}\cdot\cos\left(\frac{\gamma\pi}{6}\right)$

Thus,

$$\tan\delta = \left(\frac{\omega L \dfrac{I_d}{k.\cos\delta}}{V_a - \dfrac{I_d.R}{k.\cos\delta}} \right) \tag{5}$$

From equation (5), the angle δ can be determined using numerical methods. However, the range of value δ included in (2) is $[0, \frac{\gamma\pi}{6}]$. The first calculation is to set $\gamma = 0.5$, and then we can assume $\cos\delta \cong 1$.

As a result, $I_{a1} \cong \frac{I_d}{k}$ consequently, the equation (3) can be rewritten as follows

$$\delta = \arctan\left(\frac{I_d^*}{k - \dfrac{I_d^*.R}{\omega L}} \right) = \arctan\left(\frac{1}{\dfrac{k}{I_d^*} - \dfrac{R}{\omega L}} \right) \tag{6}$$

where $I_d^* = \frac{I_d \omega L}{V_a}$ is the normalized output dc current

As a result, the dc voltage can be kept stable by varying under equation (6).

Using the Fig. 3 (b), the input inductance and input resistance can be easily determined under the condition (2), and we assume that $I_{a1} = I_{a1\max}$ at $\delta = \frac{\gamma\pi}{6}$, then we have the following formulas

$$L = \frac{V_a \sin\left(\frac{\gamma\pi}{6}\right)}{\omega I_{a1(\max)}} \tag{7}$$

$$R = \frac{\omega L\left(1 - \cos\left(\frac{\gamma\pi}{6}\right)\right)}{\sin\left(\frac{\gamma\pi}{6}\right)} \tag{8}$$

The expression for load characteristic which shows the relationship between the dc output voltage and output dc current can be obtained on the basis of the vectors depicted in Fig. 3 (b) and equations (1), (4).

$$V_d^* = \frac{3\pi\sqrt{\left(1 - \dfrac{RI_d^*}{\omega Lk}\right)^2 + \left(\dfrac{I_d^*}{k}\right)^2}}{\sqrt{2}\left\{2\cos\left(\frac{\gamma\pi}{6}\right) + \cos\left(\frac{\pi}{3} - \frac{\gamma\pi}{6}\right) + \cos\left(\frac{\pi}{3} + \frac{\gamma\pi}{6}\right)\right\}} \tag{9}$$

Where, V_d^* is the normalized dc output voltage.

Hence, the dc output voltage variation due to load change can be stabilized by adjusting the angle according to equation (6) with respect to the dc output current after we previously define the parameters R and L.

4. Analysis of characteristics

From the input current, we can calculate various characteristics of the considered system. Figure 3(a) shows the input current of the rectifier depends on the sinusoidal supply voltage v_a and the input voltage v_{AO}.

The analysis will be simplified if we assume that the input resistance is small and can be neglected. As a result, the equation (10) can be obtained for the circuit arrangement in Fig .3(a).

$$v_a(t) - v_{A0}(t) = \omega L \frac{di_a(t)}{d\omega t} \tag{10}$$

The Fourier expansion of v_{AO} depicted in Fig. 2 gives the following equation

$$v_{A0}(t) = \sum_{n=0}^{\infty} \frac{2V_d \sin((2n+1)\omega t)}{\pi(2n+1)}\left\{\frac{2}{3}\cos\left[(2n+1)\frac{\gamma\pi}{6}\right] + \frac{1}{3}\cos\left[(2n+1)\left(\frac{\pi}{3} - \frac{\gamma\pi}{6}\right)\right] + \frac{1}{3}\cos\left[(2n+1)\left(\frac{\pi}{3} + \frac{\gamma\pi}{6}\right)\right]\right\} \tag{11}$$

Substituting $v_{AO}(t)$ into equation (10), the input current is determined as follows:

$$i_a = a\sin(\omega t + \theta) + \sum_{n=1}^{\infty} \frac{2V_d^* \cos(2n+1)\omega t}{\pi(2n+1)^2}\left\{\frac{2}{3}\cos\left[(2n+1)\frac{\gamma\pi}{6}\right] + \frac{1}{3}\cos\left[(2n+1)\left(\frac{\pi}{3} - \frac{\gamma\pi}{6}\right)\right] + \frac{1}{3}\cos\left[(2n+1)\left(\frac{\pi}{3} + \frac{\gamma\pi}{6}\right)\right]\right\} \tag{12}$$

Where $a = \sqrt{2 + a_1^2 - 2\sqrt{2}a_1 \cos\delta}$

$$a_1 = \frac{2V_d^*}{\pi}\left\{\frac{2}{3}\cos\left(\frac{\gamma\pi}{6}\right) + \frac{1}{3}\cos\left(\frac{\pi}{3} - \frac{\gamma\pi}{6}\right) + \frac{1}{3}\cos\left(\frac{\pi}{3} + \frac{\gamma\pi}{6}\right)\right\}$$

and $\theta = \arctan\left(\frac{-\sqrt{2}\cos\delta + a_1}{\sqrt{2}\sin\delta}\right)$

The distortion factor (DF), the displacement power factor (DPF), and power factor (PF) can be calculated from equations (6), (9) and (12) by using the MathCad or Mathematica. Fig. 4 shows the characteristics DF, DPF, and PF relating to dc output current with the different values of γ.

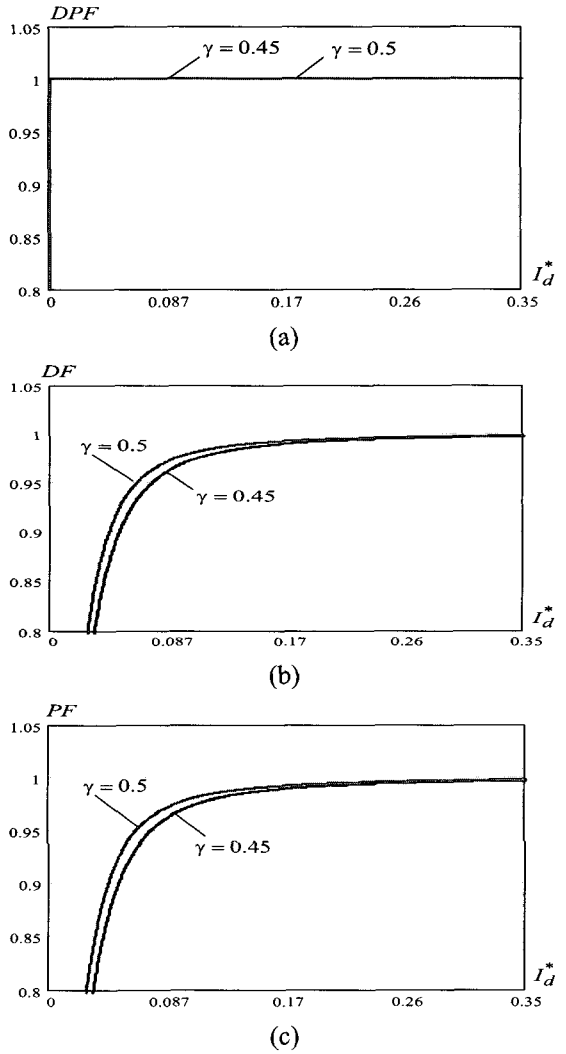

Fig. 4 Relationship between DPF, DF and PF and I_d^* under the control law of (4) with different values γ

Note that the DPF is unit but parameters DF and PF are approximately unit at light load, but it is reduced rapidly when the load is decreased. These phenomena are due to the result that the input harmonic current components become higher compared to the fundamental component. Fig. 5 shows the waveforms of the supply ac-voltage and input current drawn by using equation (12). From equation (12), it is easy to calculate the THD of the input current.

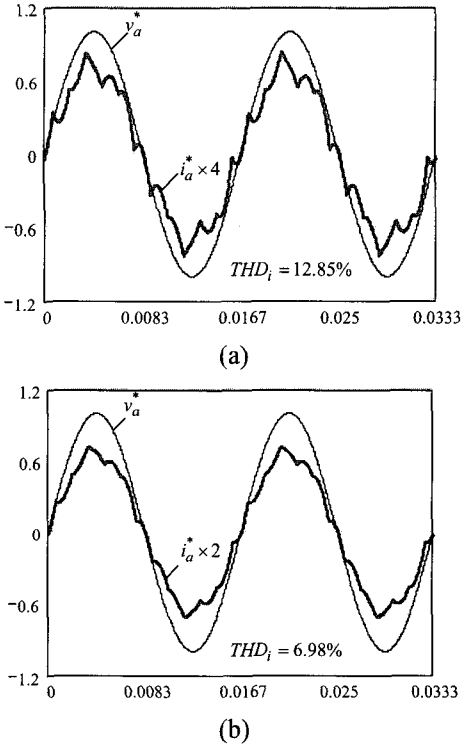

Fig. 5 The input current waveform simulated by equation 12 with respect to supply voltage v_a at $\gamma = 0.5$: (a) $I_d^* = 0.163$ and (b) $I_d^* = 0.3$

5. Simulation results

The output dc voltage can be controlled by adjusting angle δ according to equation (6). Fig. 6 shows the simulated waveforms of the supply voltage v_a, the input current i_a, the output dc voltage V_d, and the output dc current I_d. Simulations are performed under the following environments: $V_a = 95.5V$, $f = 60Hz$, $L = 3.5mH$, $R = 0.15\Omega$, $C_1 = C_2 = 1000\mu F$, and

$\gamma = 0.5$ by using Micro-Cap.

As shown in Fig. 6, the output dc voltage remains almost constant even though the load is changed quickly. As a result, we can say that the proposed rectifier has a good possibility to stabilize the output voltage under a sudden change of load. Due to this capability, the control method gives excellent sinusoidal waveforms for input current which is in co-phase with the voltage and the settling time is approximately 20 ms which is much shorter than the previous rectifier reported in [5]. A complete hardware and software implementation with experiment results is presented in the next section.

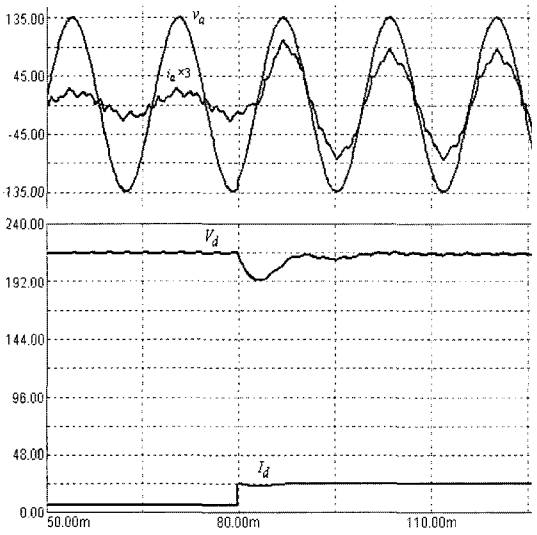

Fig. 6 Simulated results of input current i_a, supply voltage v_a, output voltage V_d, and output current I_d

6. Experimental results

The following are details of the experimental laboratory prototype described in Fig. 7: the rated output power (Pout) = 2.6KW, V_a = 95.5V, L_i = 2mH, $L_{lt} = 1.5mH$, $R = 0.15\Omega$, $C_1 = C_2 = 1000\mu F$, and utility grid frequency $f = 60Hz$.

The experiments are performed with two values of γ which are 0.45 and 0.5 utilized by the simulation program to generate a control signal for δ in the controller.

The prototype is implemented at different levels of load 0.4 kW, 0.8 kW, 1.0 kW, 1.4 kW, 1.8 kW and 2.6 kW.

The control algorithm is performed with a closed-loop as shown in Fig. 8 with the γ, L, R fixed in the control system by using an Atmel microcontroller ATMEGA8535. The output current is continuously measured in order to give the feedback value Id used for calculation of in (4) in order to produce the proposed phase shift to control the additional switches. In addition, choosing a suitable induction L is absolutely important because this will directly affect the quality of the input current and total harmonic distortion as well as the power factor.

The data are collected by oscilloscope LeCroy, using Matlab and MathCad to build up the relationship between PF and I_d^* in Fig. 11.

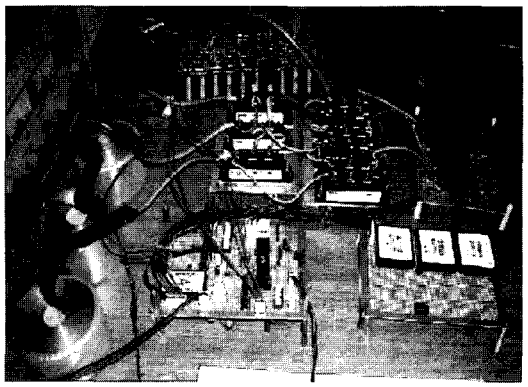

Fig. 7 Experiment prototype in laboratory

6.1 Effect of value γ to power factor

According to the simulated results in Fig 4a, 4b and 4c, it is clear that the quality of total harmonic distortion with γ = 0.5 is much better than that with γ = 0.45. The experimental results in Table 1 show that the total harmonic distortion (THD) of input current with value $\gamma = 0.45$ is much higher than that with the value $\gamma = 0.5$.

Table 1 Total harmonic distortion of the input current

P (kW)	I_d^*	THD (%), $\gamma = 0.45$	THD (%), $\gamma = 0.5$
0.4	0.025	87.69	55.3
0.8	0.05	33.70	32.22
1.0	0.063	29.29	26.87
1.4	0.088	23.32	21.00
1.8	0.113	15.98	17.50
2.6	0.163	12.32	11.94

6.2 The input power factor and current waveform of rectifier

The experimental input power factors at $\gamma = 0.5$ are presented in Table II. These results determine that the input power factor agrees with the value γ analyzed in the simulation according to Fig 4a, 4b, and 4c. The fact that using an additional switch circuit in the whole prototype and exploiting a novel control method for producing a shift control angle of bidirectional switches according to (6) really improves the power factor compared with the utility grid and reduces the total harmonics line current distortion is specifically considered and developed in this paper.

In Fig. 9, the input current i_a and the input voltage v_a are depicted. Notice that the experimental waveforms are similar to the ones obtained with the theoretical analysis which is depicted in Fig. 2.

In Fig. 10, the input current and voltage waveforms are in phase together, so that means the DPF is near unit with the considered control strategy. Furthermore, Fig 10 shows that the input current is becoming a more sinusoidal wave though the loads are changed respectively. When at last the output-power of the load greatly increases, the power factor will be improved in higher power applications. Due to these novel achievements, the control method gives an excellent result with respect to the quality of the power factor of the three-phase diodes rectifiers.

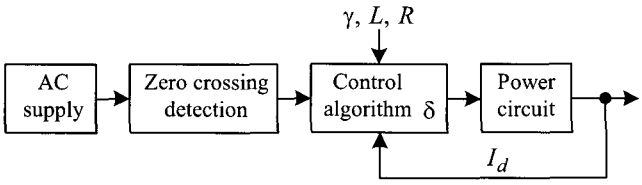

Fig. 8 The control block diagram

The proposed control strategy gives very good results as presented in Fig. 11. The power factor in the case of $\gamma =$ 0.5 shows a result very close to the simulation. The dot trace denotes results obtained by experiment and the solid line denotes results achieved by simulation analysis. The dynamic performance of this control scheme demonstrates that the input power factor of the rectifier can be improved and the THD of the input current will surely be reduced as well.

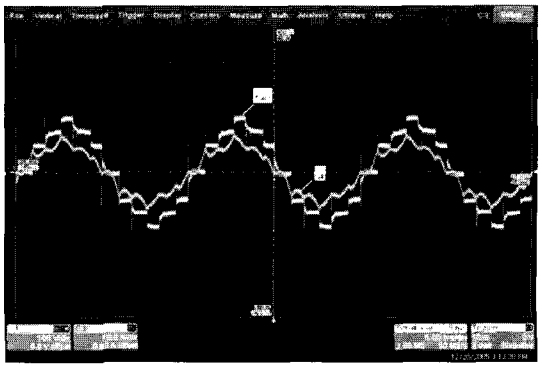

Fig. 9 The input voltage v_{AO} and current waveforms i_a

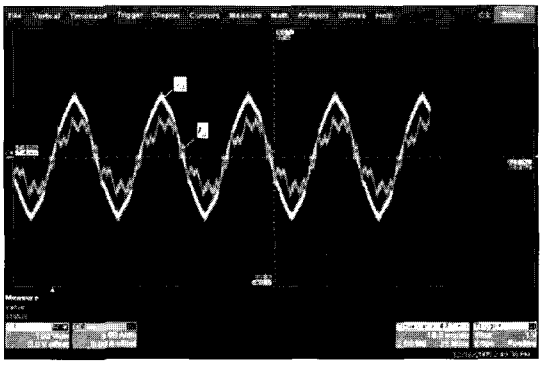

(a)

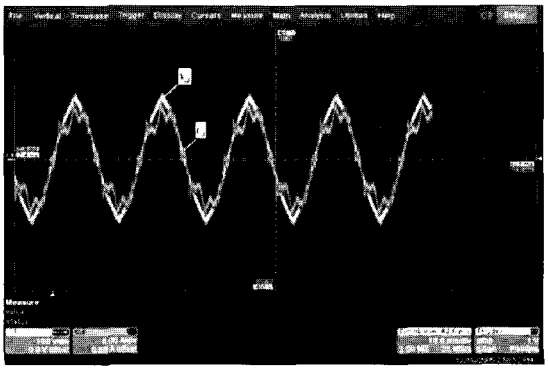

(b)

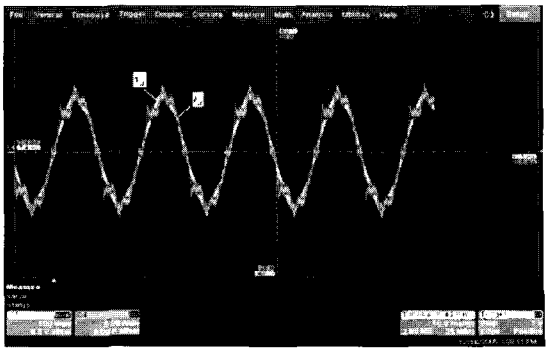

(c)

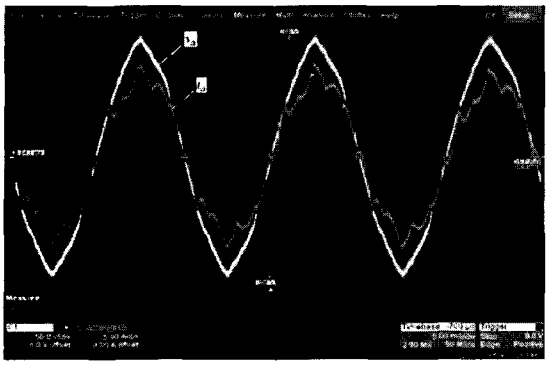

(d)

Fig. 10 The supply voltage and current waveforms with different loads at = 0.5. (a) 1.0 kW, (b) 1.4 kW, (c) 1.8 kW, (d) 2.6 kW

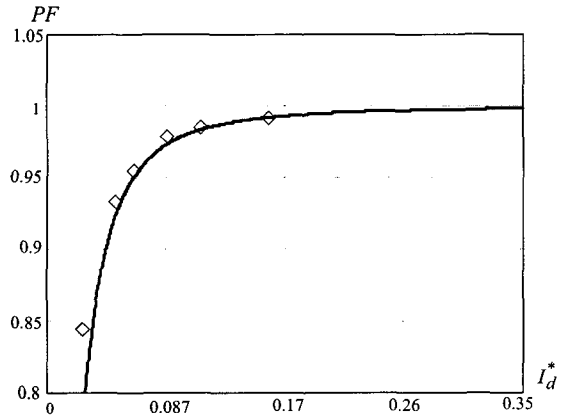

Fig. 11 Experimental and theoretical results of the power factor at value $\gamma = 0.5$ (the dot and the dash trace shows the experimental and the simulation results, respectively.)

Table 2 Input current distortion, displacement factor and power factor with different loads at $\gamma = 0.5$

P (kW)	THD (%)	cos φ	PF
0.4	55.3	0.964	0.8436
0.8	32.22	0.9801	0.9329
1.0	26.87	0.9892	0.9553
1.4	21.00	0.9999	0.9786
1.8	17.50	0.9998	0.9848
2.6	11.94	0.9985	0.9914

6.3 Stabilizing the output voltage at loads variance

The proposed control method keeps the output voltage stable even though the load is suddenly changed to different levels during operation. This is evaluated by the settling time in Fig. 12, where the settling time at the load variance from 1.0 kW to 1.8 kW is approximately 25ms. The experimental results illustrate the proposed approach has been accurately analyzed with respect to efficiency and stability.

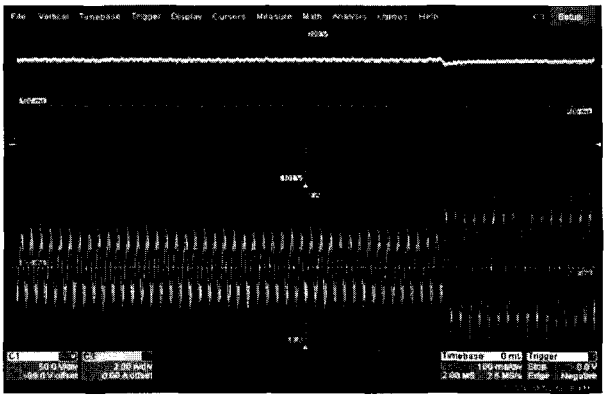

Fig. 12 Step load change from 1.0 kW to 1.8 kW; Upper trace – output dc voltage (50V/div; 100ms/div), lower trace – input current (2A/div; 100ms/div)

Fig. 13 shows the characteristics of the output dc voltage when the output current varies with the load. The dots are results obtained by experiment and the solid line is the result obtained by using equation (9). We can see that the experimental voltage is similar to the one obtained with theoretical analysis. Therefore, the experimental results fully validate the simulation and the system performance.

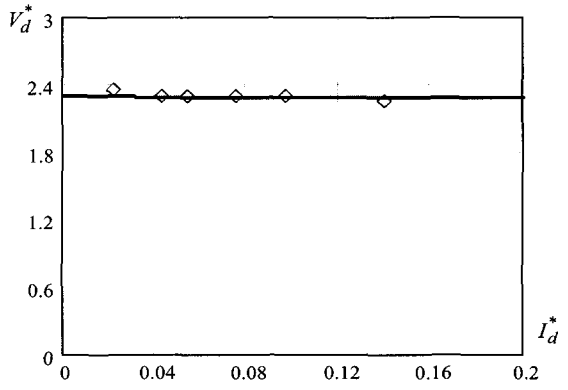

Fig. 13 Experimental and theoretical results of the dc-output voltage in versus output current

7. Conclusions

In this paper, a proposed novel control method for a diode three-phase rectifier has been presented. By choosing the different values of γ appropriately, various characteristics of DF, DPF, and PF can be achieved with respect to dc current and the output voltage, which can be stabilized at the same time under various loads. As a result, the proposed control method is able to improve the power factor of the three-phase rectifier connected with grid unity, increase the quality of the harmonics of the input current, and stabilize the output voltage. Furthermore, with the low-frequency of switches, the losses of prototype are reduced, thus the overall efficiency is increased. The considered power circuit is very suitable for implementation as a stiff voltage source.

Acknowledgment

The authors would like to thank the University of Ulsan and the MOCIE of the Korean government which partly supported this research through the Network-based Automation Research Center (NARC).

References

[1] A. R. Prasad, Phoivos D. Ziogas, Stefanos Manias, "An Active Power Factor Correction Technique Three_phase Diode Rectifiers", IEEE Transactions on Power Electronics, Vol. 6, NO.1, pp. 83-92, Jan 1991.

[2] R. Naik, M. Rastogi, and N. Mohan, "Third-harmonic modulated power electronics interface with three-phase utility to provide a regulated DC output and to minimize line-current harmonics", in IEEE Transactions on Industrial Applications, pp. 598-601 Vol.31, May-June 1995.

[3] Juan Carlos Meza, Abldu H. Samra, "The New Technique to reduce line-current Harmonics Generated by a Three-Phase Bridge Rectifier", in Proceedings of the 1998 Southeastcon, 10.1109/SECON, pp. 315-320.

[4] Nobukazu Hoshi, Tsuguhiro Tanaka, Tomotsugu Kubota, Kuniomi Oguchi, Kenichi Sakakibara, "A Novel PWM Method of Three-Phase Rectifiers for Controlling Input-Current Harmonics at Lower Switching Frequencies", Industry Applications Conference, 2001 IEEE, pp. 611-618.

[5] Joanna Aboin Gomes Marafao, Jose Antenor Pomilo, Giorgio Spiazzi "Improved Three-Phase High-Quality Rectifier With Line-Commutated Switches", IEEE Transactions on Power Electronics, Vol. 19, NO.3, pp. 640-648, May 2004.

[6] Kuniomi Oguchi, Yasuomi Maki, "Multilevel-Voltage Source Rectifier with a Three-Phase Diode Bridge Circuit as a Main Power Circuit", IEEE Transactions on Industry Applications, Vol. 30, NO.2, pp. 413-422, March/April 1994.

[7] Ewaldo L, M. Melh, Ivo Barbi, "An Improved High-Power Factor and Low-Cost Three-Phase Rectifier", IEEE Transactions on Industry Applications, Vol. 33, NO. 2, pp. 485-492, March/April 1997.

Hong-Hee Lee (M'96) is a professor of the School of Electrical Engineering, University of Ulsan, Ulsan, Korea. He is also the Director of the Network-based Research Center (NARC). He received the B.S., M.S., and Ph.D. degrees from Seoul National University, Seoul, Korea, in 1980, 1982, and 1990, respectively. His current research interests include power electronics, network-based motor control, and control networks. He is also a member of the Institute of Electrical and Electronics Engineers (IEEE), the Korean Institute of Power Electronics (KIPE), the Korean Institute of Electrical Engineers (KIEE), and the Institute of Control, Automation, and Systems Engineers (ICASE).

Van-Tung Phan was born in Binh Dinh province, Vietnam, in 1982. He received the B.S. degrees in Electrical Engineering from the University of Technology, Ho Chi Minh city, Vietnam, in 2005. Since Sep 2005, he has been with the Department of Electrical Engineering, University of Ulsan, Korea, where he has been a graduate student pursuing a Master's Degree and Doctoral Degree. He is engaged in research on Power Electronics, Motor control, and Renewable Energy.

Brovanov Sergey was born in Novosibirsk, Russia, in 1964. He received the B.S., M.S., and Ph.D. degrees in Electrical Engineering from the Novosibirsk State Technical University (NSTU), Russia, in 1985, 1987, and 1998, respectively. From 1987 to 1996, he was a research engineer at the Department of Power Electronics, NSTU. In 2005, he visited the University of Ulsan, Ulsan, Korea, as a visiting scholar for 4 months. Since 1998, he

has been with the Department of Power Electronics, NSTU, where he is currently an associate professor.

Tae-Won Chun was born in Korea in 1959. He received the B.S. degree in Electrical Engineering from Pusan National University in 1981, and received the M.S. and Ph.D. degrees in Electrical Engineering from Seoul National University in 1983 and 1987, respectively. Since 1986, he has been a member of the faculty of the Department of Electrical Engineering, Ulsan University, where he is currently a Full Professor. His current research interests are control of electrical machines, power converter circuits, and industrial applications.